

## Analysis of different GSHP system configurations: tank and control sensor position and its influence on the system performance

C. Montagud<sup>1\*</sup>, J. Cervera-Vázquez<sup>1</sup>, J. M. Corberán<sup>1</sup>

<sup>1</sup> Instituto de Ingeniería Energética, Universitat Politècnica de València, Camino de Vera s/n, 46022 Valencia, Spain

\* Corresponding author: carmonmo@iie.upv.es

**Keywords:** Heating and cooling systems, ground source heat pump, energy efficiency, optimization.

### ABSTRACT

Geocool plant was the result of a EU project whose main purpose was to adapt ground source heat pump technology to cooling dominated areas. The installation was finally built by the end of year 2004 and it has been monitored since February 2005 until nowadays. In April 2011, in the framework of another European FP7 project, Ground-med, sensitivity analysis were undertaken in order to analyze the influence of the tank and the control sensor position in the system. The impact in the user comfort and the heat pump performance is studied. Results indicate that the best configuration that guarantees the user comfort corresponds to the tank on the supply and the control sensor at the outlet of the tank. Usually, heat pump manufacturers provide the control sensor located on the return line, which is the case of the installation analyzed in this work. Therefore, in order to control the temperature supply to the building (users) and adapt it to the thermal energy demand, a control algorithm was developed and implemented in LabVIEW. Results lead to potential energy savings.

### Nomenclature

$c_p$	Specific heat at constant pressure
$DPF_1$	Heat pump DPF
$DPF_2$	Heat pump and outdoor loop DPF
$DPF_3$	Heat pump, outdoor loop and indoor loop DPF
$DPF_4$	System DPF
$\dot{m}$	Internal circuit mass flow rate
$N$	Total number of compressors of the heat pump
$n$	State of the heat pump
$\dot{Q}_{HP}$	Heat pump capacity
$T_{outHP}$	Temperature at the outlet of the heat pump
$T_r$	Return temperature
$T_s$	Supply temperature
$T_{setting}$	Heat pump temperature setting
$\dot{W}_{comp}$	Compressor consumption
$\dot{W}_{ECP}$	External circulation pump consumption
$\dot{W}_{ICP}$	Internal circulation pump consumption
$\dot{W}_{FC}$	Fan coils consumption

$\dot{W}_{par}$	Heat pump parasitic losses consumption
$\Delta T_{db}$	Heat pump temperature dead band
$\alpha$	Partial load ratio
$\eta$	Electrical efficiency of the ICP

### Acronyms

DPF	Daily Performance Factor
ECP	External Circulation pump
GSHP	Ground Source Heat Pump
ICP	Internal Circulation Pump

### 1. INTRODUCTION

Geothermal energy is becoming all around Europe one of the most interesting sources of renewable energy for heating and cooling by means of ground source heat pumps (GSHP). Ground source heat pumps (Lund 2001, Sanner et al 2003, Spitzer 2005, Chua et al 2010), take advantage of shallow geothermal energy to achieve energy savings up to 40% in comparison with conventional air to water heat pumps (Urchueguía et al 2008).

However, a good performance of these systems starts with a proper design of all its components. Particularly, the position of the buffer tank and the control sensor has not been thoroughly studied in the reviewed scientific literature. Karlsson and Fahlén (2008) analyzed different connection principles when using a dynamic model to compare capacity controlled heat pumps and intermittently controlled heat pumps. In the PhD work of Pardo García (2009), the position of a thermal storage device was analyzed, but not that of a buffer tank which provides thermal inertia to the system.

The present paper is based on a geothermal installation located in an institutional building at the Universitat Politècnica de València. Some studies undertaken during the Geocool project (Montagud et al 2011) based on the same installation were carried out with both the buffer tank and the control sensor positioned on the return line, being the control sensor at the outlet of the tank (Urchueguía et al 2008, Magraner et al 2010). Nevertheless, once the Ground-med project started (Montagud and Corberán 2010), the design of the hydraulic system had to be reconsidered as part of one of its work packages

(Work Package 5) dedicated to the “Integrated system engineering design”.

The present paper aims at the study of the influence of the buffer tank and the control sensor position on the performance of a ground source heat pump system. A mathematical model previously developed by the authors (Corberán et al 2011) was adapted to new specifications given by Ground-med project and utilized in the present work in order to perform the study.

## 2. METHODOLOGY

### 2.1 Different connection principles

Fig. 1 shows the geothermal system considered in the present work.

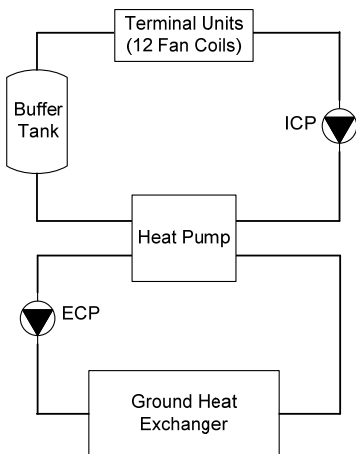


Figure 1: GSHP installation schematic diagram.

As it can be observed in Fig. 1, the installation consists of a reversible water to water heat pump, a vertical borehole heat exchanger and a hydraulic group. The system can be divided into two circuits, an external loop which carries the water down to the boreholes and back to the heat pump, and an internal loop which supplies chilled/hot water to the building where 12 fan coil units air-condition the corresponding offices. Two frequency inverters, one for each circulation pump (ICP and ECP), were installed in order to vary the internal and external circuit water flow rates. In the following, only the internal loop will be considered for the current study.

In the diagram of Fig. 1 the buffer tank has been drawn on the supply line. Nonetheless, as mentioned above, there are different possibilities when facing the positioning of both the buffer tank and the control sensor. Table 1 shows the different connection possibilities for the buffer tank and the control sensor.

Table 1: Possibilities for buffer tank and control sensor position.

Control sensor	Supply	Return
Buffer tank		
Supply	1	2
Return	3	4

For a start, option 3, which is controlling on the supply while the buffer tank is located on the return line, must be discarded because the temperature at this point may vary instantaneously during the heat pump start and stop. This instability on the temperature control probe would result in undesired effects, such as excessive cycling of the compressor.

The three remaining options are all viable since all of them present an adequate thermal inertia, whether it is provided by the buffer tank, the hydraulic circuit volume or both of them, which absorb quick variations in the controlled temperature. In the following sections, these different configurations are analyzed and compared, trying to highlight advantages and disadvantages for each one of them. It must be noticed that, even though the whole analysis is performed for cooling mode, the conclusions are applicable for heating mode.

### 2.2 What manufacturers do

Heat pump manufacturers are mostly concerned about the lifespan of their machines. Variations on the building thermal load make the temperature of the water returning to the heat pump present some quick fluctuations which may influence the compressor operation conditions and may result in lifespan shortening. That is the reason why they often include the buffer tank in the own heat pump case, locate the temperature control probe at the outlet of the tank and program the control board in such a way that only controlling on the return line is possible (as mentioned above, it would not be possible to control on the supply line if the tank is on the return line). In this way, the possible fluctuations on the return temperature due to building thermal load variations (caused, for instance, by fan coils manipulation by users) will be absorbed by the buffer tank and only stable values of temperature will appear on the return line of the heat pump.

Nonetheless, as it will be demonstrated below, this is not always the best approach as far as the user comfort is concerned. Moreover, variations in the thermal load are not going to be really high during the same day and, in any case, the volume of water contained in the piping system should be enough to absorb such small fluctuations.

It must be said that the present study has been carried out for a one-single compressor heat pump. The current installation includes a heat pump with two compressors working in tandem. The analysis with this new heat pump will be carried out and published in future works.

### 2.3 Buffer tank position when the control sensor is on the return line

In this section options 2 and 4 are compared (see Table 1). As Fig. 2 depicts, the control sensor is located on the return line following the guidelines of heat pump manufacturers, while an analysis is

undertaken in order to decide where to locate the buffer tank.

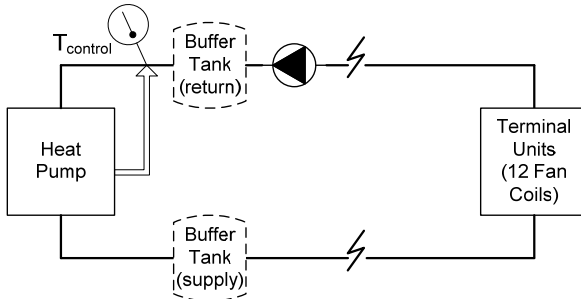


Figure 2: Control sensor located on the return line.

Several simulations were carried out in order to compare the energy performance of the system when the buffer tank is on the supply line (option 2) and when it is located on the return line (option 4). Fig. 3 shows the results of two of those simulations for a typical cooling day. In both simulations all equations and parameters (including the temperature setting) in the simulation model were the same, except for the location of the buffer tank, which was tested to be on the return or the supply line.

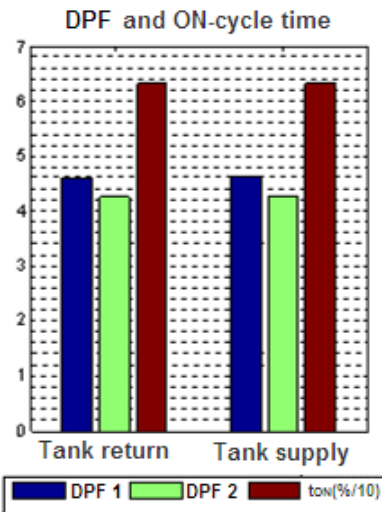


Figure 3: Tank return vs. tank supply.

The values of  $DPF_1$  (the heat pump daily performance factor) and  $DPF_2$  (which considers both, the heat pump and the external circulation pump consumption) presented in Fig. 3 are calculated using expressions [1] and [2] (considering the operational time of the installation during one whole day, that is to say 15 hours, as the integration period). The ON time ( $t_{on}(\%/10)$ ), which represent the time during which the heat pump is running (and so is the external pump, since both work simultaneously), is given in percentage of the total daily operating time (15 hours).  $\dot{W}_{par}$  represents the parasitic losses due to the electrical consumption of the electronic components of the heat pump, which has been measured and take a value of 60W approximately.

$$DPF_1 = \frac{\int_0^t \dot{Q}_{HP}(t) \cdot dt}{\int_0^t (\dot{W}_{comp}(t) + \dot{W}_{par}(t)) \cdot dt} \quad [1]$$

$$DPF_2 = \frac{\int_0^t \dot{Q}_{HP}(t) \cdot dt}{\int_0^t (\dot{W}_{comp}(t) + \dot{W}_{par}(t) + \dot{W}_{ECP}(t)) \cdot dt} \quad [2]$$

Results in Fig. 3 confirm that the installation is running during the same number of hours and the daily performance factors coincide no matter where the buffer tank is located. In reality, there is a slightly better performance factor when the tank is located on the supply line which is barely perceptible in Fig. 3.

Therefore it must be concluded that, since in both cases the energy performance of the system is really similar, it would be better to locate the tank on the supply line because it allows locating the control sensor in either, the supply or the return line. On the contrary, it would only be possible to control on the return line, as it was explained in section 2.1.

#### 2.4 Control sensor position when the buffer tank is on the supply line

In this section options 1 and 2 from Table 1 are compared. As Fig. 4 depicts, the buffer tank is located on the supply line and an analysis is carried out in order to decide where to locate the control sensor.

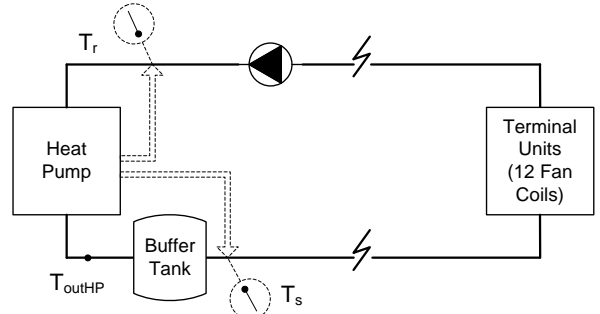
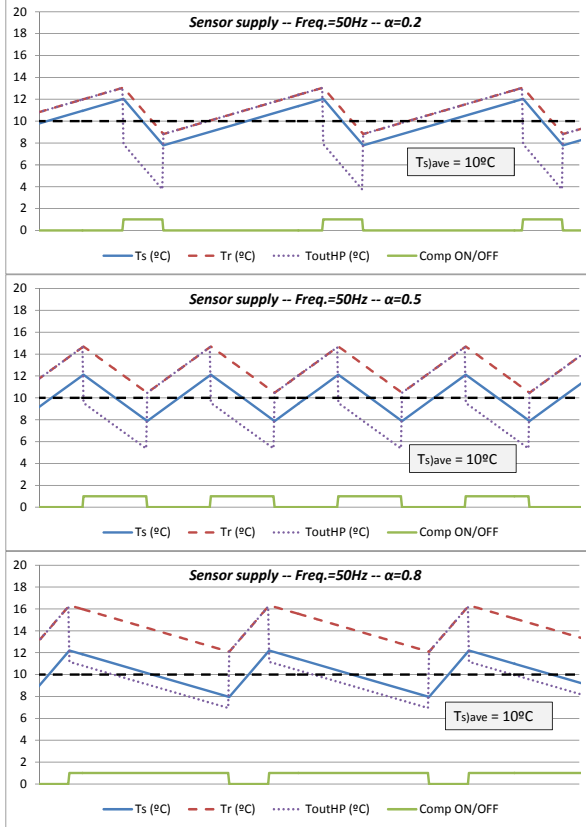


Figure 4: Tank located on the supply line.

First of all, it should be noted that both, the water flow rate and the thermal load of the building have an influence on the performance of the system. That is the reason why sensitivity analysis are undertaken and the evolution of the internal circuit temperatures with time is analyzed. These sensitivity analysis consist of varying one parameter (the one whose influence is analyzed) while the rest are kept constant. Regarding the flow rate, since the installation studied allows variable frequencies for the circulation pumps, the effect of varying the flow rate is studied. With respect to the thermal load, it is taken into account by means of the load ratio ( $\alpha$ ), which is the relation between the instantaneous thermal load of the building and the heat pump capacity (always higher than the thermal load). Therefore, small thermal loads will result in values of  $\alpha$  close to zero, and higher thermal loads will give values of  $\alpha$  close to one. In the following, results are only presented for cooling mode.

Fig. 5 depicts the results of several simulations for different values of the load ratio ( $\alpha = 0.2$ ,  $\alpha = 0.5$  and  $\alpha = 0.8$ ) keeping constant the frequency at 50Hz. The temperature setting considered in all three cases is the same, 10°C, with temperature dead band of  $\pm 2^\circ C$ . The figure shows the time evolution of the

temperature at the outlet of the heat pump ( $T_{outHP}$ ), at the outlet of the buffer tank, that is the temperature of the water supplied to the building ( $T_s$ ) and the temperature at the inlet of the heat pump, that is the temperature of the water returning from the building ( $T_r$ ). In addition, the ON/OFF signal of the compressor is also plotted in order to be able to follow the heat pump operation (1 = *ON*; 0 = *OFF*).



**Figure 5: Internal circuit temperatures for different values of  $\alpha$  (from top to bottom:  $\alpha = 0.2$ ,  $\alpha = 0.5$  and  $\alpha = 0.8$ ) with control sensor on supply line.**

The same time scale is considered in all three graphs in Fig. 5. Focusing on the signal “Comp ON/OFF”, the influence of the load ratio can be observed, since the higher the value of  $\alpha$ , the longer the time during which the compressor is running; which makes sense, because it takes longer for the heat pump to cool down the water when the thermal demand is higher. The compressor cycles can also be detected through the temperature at the outlet of the heat pump ( $T_{outHP}$ ), since it coincides with the return temperature ( $T_r$ ) when the compressor is off, but takes values around 5°C lower when the compressor is running.

It can also be observed that the average value of the supply building temperature ( $T_s)_{ave}$ ) remains constant and equal to 10°C no matter the value of the load ratio. Results are redundant in the case of applying a frequency of 20Hz. It is important to realize that this is really beneficial because the water at the inlet of the fan coils only present the variation corresponding to the dead band of the heat pump controller ( $\pm 2^\circ\text{C}$  in the example of Fig. 5), being the average temperature

the same during all the operation period. Therefore, the heating/cooling capacity of the fan coils will not be affected by a variation in the inlet temperature and will be more stable which is better for user comfort.

On the contrary, when the control sensor is located on the return line (keeping the same temperature setting and dead band of  $10 \pm 2^\circ\text{C}$ ), which is the case for the simulation results shown in Fig. 6, it can be observed that the higher the load ratio, the lower the average value of the temperature supplied to the building, which means that the higher the thermal load, the lower the temperature of the water supplied to the building. This influence is given by expression [3].

$$T_s)_{ave} = T_r)_{ave} - \alpha \cdot \frac{\dot{Q}_{HP}}{m \cdot c_p} \quad [3]$$

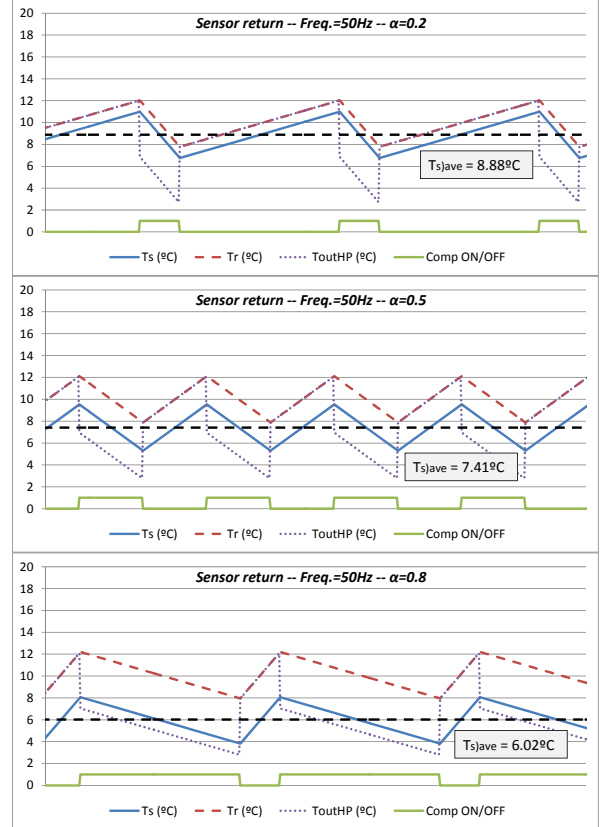


**Figure 6: Internal circuit temperatures for different values of  $\alpha$  (from top to bottom:  $\alpha = 0.2$ ,  $\alpha = 0.5$  and  $\alpha = 0.8$ ) with control sensor on return line.**

Regarding the influence of the frequency (and hence the flow rate), as previously presented, there are two frequency inverters in order to vary the flow rate in the hydraulic circuits. For that reason, the influence of the flow rate variation must be also studied.

For small thermal loads, low frequencies will be applied. Lower frequencies mean lower flow rates and, according to expression [3], lower frequencies will result in lower temperatures of the water supplied to the building ( $T_s)_{ave}$ ). Therefore, the performance would be worse for small loads. Taking for instance a value of 0.2 for the load ratio, Fig. 7 shows the temperatures evolution with time for 50Hz and 20Hz.

As it can be observed, when different frequencies are used, keeping the same temperature setting and dead band as previously ( $10 \pm 2^\circ\text{C}$ ), the average temperature of the water supplied to the building ( $T_{s,\text{ave}}$ ) is not the same. Therefore, if the frequency is varied during the day as part of an integrated optimization algorithm, the user comfort could be affected if the control sensor is located on the return line.

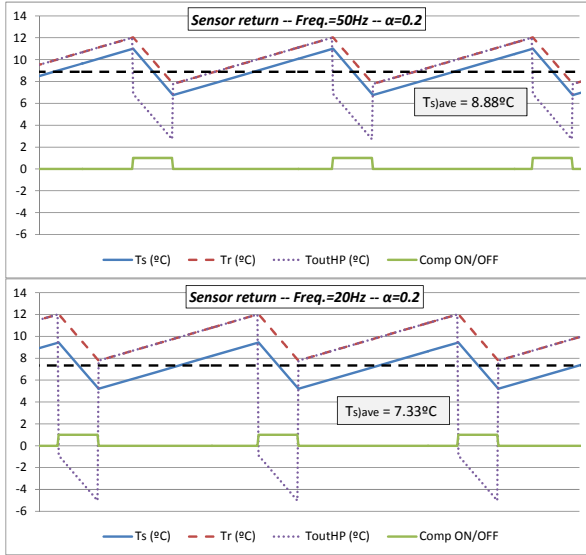


**Figure 7: Internal circuit temperatures for different values of frequency (top:  $\text{freq} = 50\text{Hz}$ , bottom:  $\text{freq} = 20\text{Hz}$ ) with control sensor on return line.**

In addition, the graph on the bottom in Fig. 7 shows up the possibility of having freezing problems when the frequency is varied. For higher values of  $\alpha$  this performance would be even worse. Therefore, the heat pump must include anti-freezing alarm. Besides, the temperature setting should be readjusted when small frequencies are applied in order to avoid these freezing problems. Although results for a frequency of 20Hz with the control sensor on the supply line are not shown in the present work, the same performance was observed in that case.

To sum up, when the control sensor is located on the return line, the temperature of the water supplied to the building may suffer strong variations which may result in a degradation of the user comfort. Therefore it must be concluded that, from the point of view of the user comfort, it is better to locate the control sensor on the supply line.

Up to now, only the user comfort has been analyzed in order to decide which is the best location for the control sensor, whether the supply or the return line. Nevertheless, when it comes to the energy performance of the system, results are not so clear.

Fig. 8 shows the same results as Fig. 3 but compares the energy performance for options 1 and 2 (according to Table 1) for a typical cooling day. Results are favorable for option 1 (sensor supply) whose performance factor is better. However, this is just

because, since the temperature setting considered is the same in both cases, due to the position of the sensor the water must be cooled down to a lower temperature when the control sensor is on the return line.

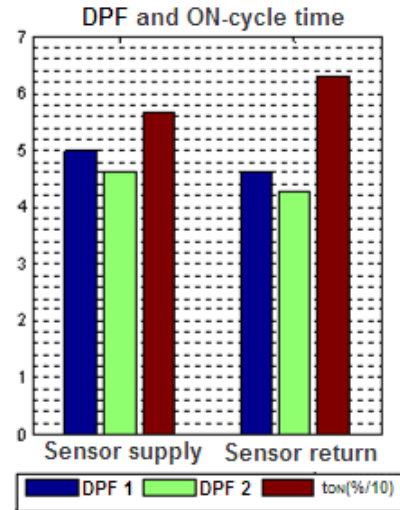


**Figure 8: Sensor supply vs. sensor return.**

Let us look, for instance, at the  $\alpha = 0.5$  graphs in Fig. 5 and Fig. 6. In Fig. 5 (sensor supply) the water is cooled down to  $10^\circ\text{C}$  ( $T_{s,\text{ave}}$ ). However, when the sensor is on the return (Fig. 6), it is the return temperature that is kept at  $10^\circ\text{C}$  ( $T_{r,\text{ave}}$ ), while the supply water is cooled down to  $T_{s,\text{ave}} = 7.41^\circ\text{C}$ , resulting in an extra energy consumption which deteriorates the performance factor.

Therefore, the energy performance cannot be used as a decision factor because, if a temperature setting readjustment was applied which achieves that the supply temperature remains constant, the energy performance of both options (sensor supply and sensor return) would be very similar. This setting readjustment is applied as part of an optimization algorithm which will be explained in the following section.

At this point it can be concluded that, when the buffer tank is located on the supply line, the best configuration from the point of view of the user comfort is to locate the control sensor on the supply line, at the outlet of the tank. In this way, the temperature of the water sent to the building will always have the same average temperature, which means comfort for the user.

## 2.5 Integrated optimization algorithm

In sections 2.3 and 2.4 it was concluded that, from the point of view of the user comfort, the best position for both the buffer tank and the control sensor is the supply line. The buffer tank was located on the supply line without any problems. However, the heat pump in the installation was programmed in such a way that only controlling on the return line was possible. As it was said in section 2.2, that is what most

manufacturers do. Therefore, the control sensor had to remain on the return line.

As explained in the previous section, this may cause some problems. Fig. 9 shows how, depending on the thermal load of the building (represented by  $\alpha$ ) and the flow rate of water (represented by the frequency), the supply building temperature varies (according to expression [3]). As it can be seen, whereas the average return temperature ( $T_{r,ave}$ ) remains constant because it is the controlled temperature (notice the setting would be 10°C), the higher the load ratio ( $\alpha$ ), the lower the average temperature of the water supplied to the building ( $T_{s,ave}$ ). On the other hand, the lower the frequency, that is to say the lower the flow rate, the lower the average temperature of the water supplied to the building.

Nonetheless, the authors' aim is to control the temperature of the water supplied to the building. For that purpose, a correction could be introduced in the temperature setting of the heat pump (measured on the return) which takes into account the variations in the thermal load and the flow rate, in order to maintain constant the supply building temperature. Fig. 9 also makes clear the freezing problem for low frequencies mentioned in the previous section.

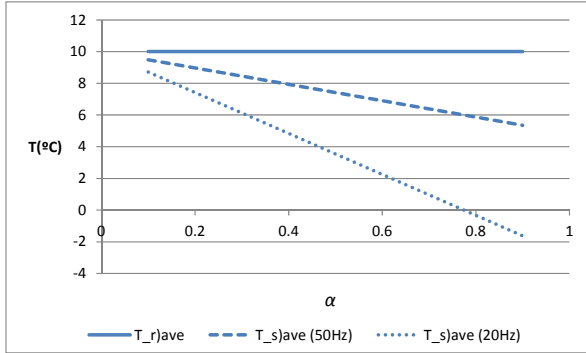


**Figure 9: Variation of the supply building temperature with  $\alpha$  and the frequency.**

In the following, a brief summary of the integrated optimization algorithm developed by the authors in order to take into account the considerations stated in the above paragraph is introduced and some preliminary results obtained for heating mode are presented. Further details and results regarding the integrated optimization of the system will be published in future works.

For a start, Table 2 shows the controlled variables and control parameters involved in the optimization algorithm.

The algorithm includes the variation of the circulation pumps frequencies (mentioned at some points of the present work) in order to optimize the energy performance of the system.

**Table 2: Controlled variables and control parameters.**

CONTROLLED VARIABLES		
$\dot{m} = \dot{m}(ICP_{freq})$		$T_{s,ave}$
CONTROL PARAMETERS		
$T_{setting}$	$\Delta T_{db} = \frac{Differential}{N}$	$ICP_{freq}$

Therefore, as expression [4] shows, the internal circuit flow rate ( $\dot{m}$ ) must be determined as a function of the load ratio of the system ( $\alpha$ ) as well as the season or mode, which can be cooling or heating mode. The entire optimization methodology can be found in Montagud et al (unpublished results) and a summary is presented in Montagud et al (unpublished results, 2013).

$$\dot{m} = \dot{m}(ICP_{freq}) = f(season, \alpha) \quad [4]$$

Moreover, the algorithm also considers temperature compensation in such a way that, as expression [5] shows, the supply building temperature is set according to the ambient temperature.

$$T_{s,ave} = f(season, T_{amb}) \quad [5]$$

In order to control these variables, the parameters that can be controlled, by means of an application implemented in LabVIEW, correspond to the circulation pump frequency ( $ICP_{freq}$ ), through a frequency inverter, and the temperature setting ( $T_{setting}$ ) and dead band ( $\Delta T_{db}$ ) of the heat pump, by sending the values to the heat pump electronic controller.

For the time being, the heat pump dead band is not being varied during the experiments, but kept at a constant value. Regarding the heat pump temperature setting, after considering some specific conditions of the heat pump and doing some calculations, expression [6] was obtained in order to calculate a value of the temperature setting so that the average value of the temperature of the water supplied to the building remains constant and equal to the value calculated by the temperature compensation (expression [5]).

$$T_{setting} = T_{s,ave} + \Delta T_{db} \cdot \left( n - \frac{1}{2} \right) - \frac{\alpha \cdot \dot{Q}_B}{\dot{m} \cdot c_p} \quad [6]$$

Equation [6] is for heating mode. For cooling mode the expression is the same but changing the signs of the two last addends. This temperature setting is recalculated at the end of each complete cycle of the heat pump and sent to the heat pump controller. As it was mentioned above, further details regarding the algorithm development will be published in future works.

Fig. 10 shows an example of experimental results of applying the optimization algorithm during a whole typical heating day. The values of the temperatures can be observed on the left hand axis whereas the compressor power is represented on the right hand axis.

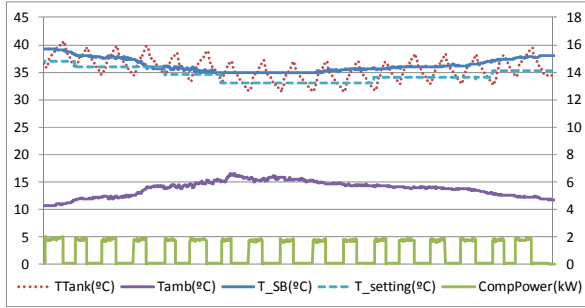


**Figure 10: Optimization algorithm experimental results (heating mode).**

From the temperature compensation, the desired supply building temperature ( $T_{SB}$ ) is inversely proportional to the ambient temperature ( $T_{amb}$ ). Variations of the ambient temperature from 10 to 15°C result in values of the desired supply building temperature from 40 to 35°C approximately. As it can be observed in Fig. 10, the real temperature of the water supplied to the building measured at the outlet of the buffer tank ( $T_{Tank}$ ) follows fairly accurately the wanted supply building temperature ( $T_{SB}$ ). It must be remarked that this performance is achieved by varying the temperature setting ( $T_{setting}$  in Fig. 10) of the heat pump according to expression [6]. In this way, the water is supplied to the building at the desired temperature at each moment according to the external ambient conditions.

This operation together with the flow rate control of both the external and the internal hydraulic circuit, result in the end in a considerable improvement of the energy performance of the system. This improvement on the system energy performance can be assessed by calculating different performance factors and comparing an optimized day to a day when standard control was applied. This standard control would correspond to standard values for the control parameters, that is to say 40°C as the temperature setting (13°C for cooling mode) and a frequency of 50Hz for both circulation pumps. The value of the temperature setting (40°C) may be a little bit low when comparing standard applications in the market (above 45°C). The reason for this is that, due to specific requirements of Ground-med project, the maximum return temperature must be 40°C. The improvements shown later on would be even better if results were compared to standard applications in the market.

Fig. 11 shows experimental results of applying the optimization algorithm regarding the energy savings when compared to a standard control. The performance of the system is analyzed by means of following daily performance factors: the heat pump

DPF ( $DPF_1$ ) and the heat pump and external circuit DPF ( $DPF_2$ ) as calculated by equations [1] and [2], the one considering both the heat pump consumption and the external and internal pumps consumption ( $DPF_3$ ), as determined by equation [7], and the system DPF ( $DPF_4$ ), which also takes the fan coils consumption into consideration [8].

$$DPF_3 = \frac{\int_0^t (\dot{Q}_{HP}(t) + \eta \cdot \dot{W}_{ICP}(t)) \cdot dt}{\int_0^t (\dot{W}_{comp}(t) + \dot{W}_{par}(t) + \dot{W}_{ECP}(t) + \dot{W}_{ICP}(t)) \cdot dt} \quad [7]$$

$$DPF_4 = \frac{\int_0^{t_{ON}} (\dot{Q}_{HP}(t) + \eta \cdot \dot{W}_{ICP}(t)) \cdot dt}{\int_0^{t_{ON}} (\dot{W}_{comp}(t) + \dot{W}_{par}(t) + \dot{W}_{ECP}(t) + \dot{W}_{ICP}(t) + \dot{W}_{FC}(t)) \cdot dt} \quad [8]$$

The period considered for the integration corresponds to the operational time of the installation during one whole day, that is to say 15 hours.  $\dot{W}_{ICP}$  and  $\dot{W}_{FC}$  are the internal circulation pump and fan coils electrical consumption respectively. It must be noticed that the operation of the internal circulation pump heats up the water on the internal circuit, that is the reason why its consumption appears in the numerator in equations [7] and [8] multiplied by the corresponding electrical efficiency. In cooling mode there should be a negative sign. See Montagud et al (unpublished results) for further details.

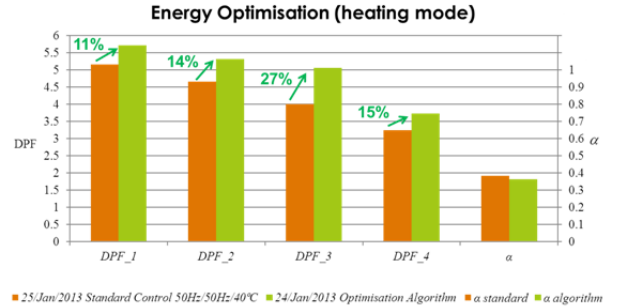


**Figure 11: Energy performance improvement by applying the optimization algorithm.**

Fig. 11 shows, from left to right, performance factors from 1 to 4. The last couple of bars confirm that the average load ratios ( $\alpha$ ) of both the standard and the optimized day are really similar, around 0.38, which makes it possible to make a fair comparison. As it can be observed, the improvement can be noticed in all performance factors and the percentages of improvement are also presented in Fig. 11. Nonetheless, the system DPF ( $DPF_4$ ) is the most representative one, since it takes into consideration the overall energy performance of the system. Therefore, according to the experimental results, around 15% of energy savings could be obtained by applying the optimization algorithm.

In any case, it must be pointed out that  $DPF_3$  presents fairly higher energy savings, up to 27%. However, the degradation of the energy savings when it comes to  $DPF_4$  might be due to the poor performance of the fan coils installed in the facility. Future studies could analyze the energy performance of the system after applying the optimization algorithm in case the old fan

coils were replaced with a more modern and efficient design ones.

### 3. CONCLUSIONS

The influence of the position of the buffer tank and the control sensor on the user comfort and the energy performance of a ground source heat pump installation is studied in the present paper. Different configurations are possible for both components.

First of all, the position of the buffer tank is studied when the control sensor is located on the return line. Whether the tank is located on the supply or the return line the energy performance of the system is really similar. Therefore, it is decided that the buffer tank should be located on the supply line because that would allow locating the control sensor in either, the supply or the return line. On the contrary, it would only be possible to control on the return line.

Second, considering the buffer tank located on the supply line, the influence of the position of the control sensor is analyzed. It is concluded that from the point of view of the user comfort, the best configuration is to locate the control sensor on the supply line, at the outlet of the tank. In this way, the temperature of the water sent to the building will always have the same average temperature, which means comfort for the user.

Therefore, the best approach would be to locate both the buffer tank and the control sensor on the supply line. However, the heat pump in the installation is internally programmed in such a way that only controlling on the return line is possible, hence the control sensor must remain on the return line.

For that reason, in order to be able to control the temperature of the water supplied to the building, an integrated optimization algorithm is developed and implemented in LabVIEW. The desired supply building temperature is achieved by varying the temperature setting applied to the heat pump as a function of the ambient temperature and the thermal load. The integrated optimization algorithm also includes the variation of the circulation pumps frequencies in order to save energy when the thermal load is small by reducing the frequencies of the circulation pumps by means of frequency inverters. Preliminary experimental results are presented. They show considerable energy savings, up to 15% for heating mode. Further research will be carried out in order to optimize the operation of the fan coil units as they have been proved of having a great influence in the global energy savings ( $DPF_3$  vs.  $DPF_4$  in Fig. 11).

### REFERENCES

Lund, J.W.: Geothermal heat pumps – an overview, *Geo-Heat Center Bulletin*, **22(1)**, (March, 2001), 1-2.

Sanner, B., Karytsas, C., Mendrinos D. and Rybach, L.: Current status of ground source heat pumps and underground thermal storage in Europe, *Geothermics*, **32(4-6)**, (2003), 579-588.

Spitler, J.D.: Ground-Source Heat Pump System Research – Past, Present and Future, *Europe, HVAC&R Research*, **11(2)**, (2005), 165-167.

Chua, K.J., Chou, S.K. and Yang, W.M.: Advances in heat pump systems: A review, *Applied Energy*, **87(12)**, (2010), 3611-3624.

Urchueguía, J.F., Zacarés, M., Corberán, J.M., Montero, Á., Martos, J. and Witte, H.: Comparison between the energy performance of a group coupled water to water heat pump system and an air to water heat pump system for heating and cooling in typical conditions of the European Mediterranean Coast, *Energy Conversion and Management*, **49(10)**, (2008), 2917-2923.

Karlsson, F. and Fahlén, P.: Impact of design and thermal inertia on the energy saving potential of capacity controlled heat pump heating systems, *International Journal of Refrigeration*, **31**, (2008), 1094-1103.

Pardo García, N.: Energy efficiency improvement of hybrid ground coupled HVAC systems from thermal energy generation and storage management, *PhD Thesis at Universitat Politècnica de València*, Valencia, (2009)

Montagud, C., Corberán, J.M., Montero, Á. and Urchueguía, J.F.: Analysis of the energy performance of a ground source heat pump system after five years of operation, *Energy and Buildings*, **43(12)**, (2011), 3618-3626.

Urchueguía, J.F., Zacarés, M., Corberán, J.M., Montero, Á., Martos, J. and Witte, H.: Comparison between the energy performance of a ground coupled water to water heat pump system and an air to water heat pump system for heating and cooling in typical conditions of the European Mediterranean coast, *Energy Conversion and Management*, **49**, (2008), 2917-2923.

Magraner, T., Montero, Á., Quilis, S. and Urchueguía, J.F.: Comparison between design and actual energy performance of a HVAC-ground coupled heat pump system in cooling and heating operation, *Energy and Buildings*, **42**, (2010), 1394-1401.

Montagud, C. and Corberán, J.M.: Ground-med project: advanced ground source heat pump systems for heating and cooling in Mediterranean climate, *Proceedings of the “II Congreso de Energía Geotérmica en la Edificación y la Industria (GEOENER 2010)” (Spanish)*, Madrid, Spain, (2010), 293-299.

Corberán, J.M., Finn, D.P., Montagud, C., Murphy, F.T. and Edwards, K.C.: A quasi-steady state mathematical model of an integrated ground source heat pump for building space control, *Energy and Buildings*, **43**, (2011), 82-92.

Montagud, C., Corberán, J.M. and Montero, Á.: Optimization methodology for the water circulation pumps frequency of ground source heat pump systems, (*Unpublished results*).

Montagud, C., Cervera-Vazquez, J. and Corberán, J.M.: Optimization methodology for GSHP installations based on the circulation pumps frequency variation, *European Geothermal Congress*, Pisa, Italy, (2013), (*Unpublished results*).

### **Acknowledgements**

This work was supported by the “Programa de Ayudas de Investigación y Desarrollo (PAID)” of the Universitat Politècnica de València.

This work was also supported under the FP7 programme “Advanced ground source heat pump systems for heating and cooling in Mediterranean climates” (Ground-med).